*International Journal of Astrobiology* 4 (1): 63–73 (2005) Printed in the United Kingdom
doi:10.1017/S1473550405002454 © 2005 Cambridge University Press


# Chiral polymerization and the RNA world

Jonathan A.D. Wattis[1]* and Peter V. Coveney[2]*

[1]*Theoretical Mechanics, School of Mathematical Sciences, University of Nottingham, University Park, Nottingham NG7 2RD, UK*
*e-mail: Jonathan.Wattis@nottingham.ac.uk*
[2]*Centre for Computational Science, Department of Chemistry, University College London, 20 Gordon Street, London WC1H 0AJ, UK*
*e-mail: p.v.coveney@ucl.ac.uk*

**Abstract**: The purpose of this paper is to review two mathematical models: one for the formation of homochiral polymers from an originally chirally symmetric system; and the other, to show how, in an RNA-world scenario, RNA can simultaneously act both as information storage and a catalyst for its own production. We note the similarities and differences in chemical mechanisms present in the systems. We review these two systems, analysing steady states, interesting kinetics and the stability of symmetric solutions. In both systems we show that there are ranges of parameter values where some chains increase their own concentrations faster than others.

*Received 21 March 2005, accepted 4 May 2005*

**Key words**: chiral polymerization, mathematical modelling, origins of life, RNA world.

## Introduction

The origin and propagation of molecular handedness is one signature of life, and a comprehensive and consistent description of the mechanisms by which it arose has yet to be achieved, though an excellent starting point is the discussion of Sandars (2005). Similarly, much has been written about the RNA world (for example, Colonna *et al*. 1994; Zubay 2000), and there is a large literature on catalytic hypercycles (see, for example, Eigen 1971; Eigen & Schuster 1979) yet there is little published work on how such systems arose from a simpler chemical system.

The purpose of this short article is to review and compare two models of polymerization of relevance to the origins of life, each having complex steady-state and kinetic features. The first, and slightly simpler one, is that of chiral polymerization (Wattis & Coveney 2005). This is concerned with showing that enantiomeric cross-inhibition is a driving force *for* symmetry breaking in chiral polymerization, rather than a hindering factor as had been originally thought (Joyce *et al*. 1984). This work confirms the numerical results of Sandars (2003), who originally proposed a form of the model we study, and similar supporting evidence has been found by Brandenburg *et al*. (2005a), who has also worked on generalizations of Sandars' model (see also Brandenburg *et al*. 2005b).

An original aspect of our work is that we analyse not only the stability of the steady-state solutions, but also the stability of the kinetic solution. To do this we first derive an asymptotic approximation for a *symmetric* solution. We identify and comment upon the range of behaviour displayed as it evolves in time through several timescales. Once the kinetics of the *symmetric* solution have been determined, we analyse its stability to random external perturbations. The results of this show that there are some stages of the polymerization process during which the system is more likely to undergo a symmetry-breaking bifurcation than others.

The model of chiral polymerization has the form of a generalized Becker–Döring system of equations, which have been modified in various ways to explore a number of chemical systems (Coveney & Wattis 1996, 1998). In chiral polymerization nonlinearity appears in a feedback mechanism whereby an achiral substrate breaks down into two forms of chiral monomer (denoted by $L_1$ and $R_1$). The amount of each type of monomer produced is influenced by the total amount of chiral polymer present in the system, the strength of this effect being controlled by a fidelity parameter.

The second topic we review here again uses a modified Becker–Döring scheme to model the formation of an RNA world, summarizing Wattis & Coveney (1999). Here nonlinear feedback is again of crucial importance. However, in this model the feedback does not influence the production of monomers, rather it affects the way in which monomers polymerize. Long polymers act as templates for polymerization, thus allowing information to be propagated through the system.

These two systems share common features: we have already compared and contrasted the nonlinear feedback mechanisms; however, they also exhibit competition. In chiral polymerization the chains compete for monomers and, when the rate of attachment for the monomer to the opposite

* Corresponding author.

handed polymer exceeds that of its own, then symmetry breaking is more likely. In the RNA-world model polymers again compete for monomers; and despite there being no inhibition, symmetry breaking still occurs.

In the remainder of this section we introduce the Becker–Döring system which we use as the basis for our more complicated models of polymerization discussed later. The section on chiral polymerization reviews the model and results for chiral polymerization, and the subsequent section summarizes a model for the formation of an RNA world. Important common features and differences are discussed in the conclusions section.

*The Becker–Döring system*

The Becker–Döring system of equations was originally constructed to model nucleation (Becker & Döring 1935), but has since been applied to a wide range of aggregation phenomena. It is based on modelling the spatially averaged concentrations $c_r(t)$ of clusters $C_r$ which undergo cluster–monomer aggregation (and possibly fragmentation) processes of the form

$$C_r + C_1 \rightleftharpoons C_{r+1}, \tag{1}$$

with forward rate usually denoted by $a_r$ and backward rate $b_{r+1}$ (possibly zero). The flux of material from size $r$ to $r+1$ is then given by $J_r = a_r c_r c_1 - b_{r+1} c_{r+1}$. The major assumption implicit in (1) is that cluster–cluster interactions do not occur; that is, $C_r + C_s \to C_{r+s}$ with $r > 1$ and $s > 1$ are ignored. The rate of change of concentration of clusters of size $r$ is given by

$$\frac{dc_r}{dt} = J_{r-1} - J_r. \tag{2}$$

The concentrations of most cluster sizes depends only on those of neighbouring size and the monomer. The monomer concentration is then given by

$$\frac{dc_1}{dt} = q(t) - J_1 - \sum_{r=1}^{\infty} J_r, \tag{3}$$

with $q(t)$ being the input rate of monomers, from some external or coupled system. Equation (2) is said to be at equilibrium if the fluxes $J_r$ are zero, and at steady state if the fluxes $J_r$ are non-zero but the same for all $r$.

## Chiral polymerization

*Model*

First, we summarize the work of Wattis and Coveney (2005). Our model is based on that of Sandars (2003), and shares similarities with the model studied by Brandenburg *et al.* (2005a). We are concerned with the following set of coupled chemical reactions ((4), (6)–(7)) in which an achiral substrate ($S$) is broken down into chiral monomers ($L_1$ and $R_1$) both spontaneously at a slow rate ($\varepsilon$) and at a faster rate ($k$) by a process catalysed by the presence of homochiral polymers. This catalytic feedback mechanism is partially selective, in

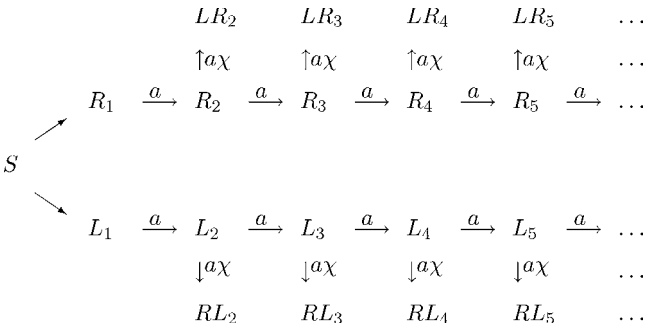


**Fig. 1.** Summary of the proposed model of chiral polymerization. All steps are straightforward additions, with the exception of the decay of the substrate $S$ into chiral monomers $L_1$ and $R_1$, which occurs by a combination of spontaneous and catalysed breakdown described by (4).

that left-handed polymers catalyse the formation of left-handed monomers more than right-handed monomers. The selectivity of this feedback is described by the fidelity parameter $f$,

$$\begin{aligned} &S \xrightarrow{\varepsilon} L_1, \quad S + Q \xrightarrow{\frac{1}{2}k(1+f)} L_1 + Q, \quad S + P \xrightarrow{\frac{1}{2}k(1-f)} L_1 + P, \\ &S \xrightarrow{\varepsilon} R_1, \quad S + P \xrightarrow{\frac{1}{2}k(1+f)} R_1 + P, \quad S + Q \xrightarrow{\frac{1}{2}k(1-f)} R_1 + Q. \end{aligned} \tag{4}$$

Here we use $L_n$ to denote a chirally pure (homochiral) left-handed polymer of length $n$ (similarly $R_n$ for right). The total numbers of polymers ($L$ and $R$) and the mass of material in each form ($Q$ and $P$) are then given by

$$L = \sum_{n=2}^{\infty} L_n, \quad R = \sum_{n=2}^{\infty} R_n, \quad Q = \sum_{n=2}^{\infty} nL_n, \quad P = \sum_{n=2}^{\infty} nR_n. \tag{5}$$

Hence (4) describes how the mass of chirally pure polymers influences the breakdown of achiral $S$ into chiral monomers $L_1$ and $R_1$. These monomers then combine to form chirally pure polymers, ($L_n$ and $R_n$) according to the usual rules for (irreversible) polymerization at a rate $a$,

$$L_n + L_1 \xrightarrow{a} L_{n+1}, \quad R_n + R_1 \xrightarrow{a} R_{n+1}. \tag{6}$$

However, by the process known as *enantiomeric cross-inhibition*, the 'wrong' monomer can attach to a chain (with rate $a\chi$) leading to a 'spoilt' polymer chain which can grow no further,

$$L_n + R_1 \xrightarrow{a\chi} RL_n, \quad R_n + L_1 \xrightarrow{a\chi} LR_n. \tag{7}$$

The scheme of chemical reactions is summarized in Fig. 1.

In considering the equations for the concentrations of quantities in the model (4)–(7), it is simpler to transform to quantities which represent the total amount of monomers ($\mu$), the total number of polymers ($N$) and the total mass of material in polymeric form ($M$) according to

$$\mu = L_1 + R_1, \quad N = L + R, \quad M = P + Q, \tag{8}$$

https://doi.org/10.1017/S1473550405002454 Published online by Cambridge University Press

and then consider separately the chiral purity of each of these quantities via

$$\delta = \frac{R_1 - L_1}{R_1 + L_1}, \quad \theta = \frac{R - L}{R + L}, \quad \eta = \frac{P - Q}{P + Q}. \tag{9}$$

The kinetic equations governing these total concentrations and purities are then

$$\frac{dS}{dt} = S_0 - 2\varepsilon S - kSM, \tag{10}$$

$$\frac{d\mu}{dt} = 2\varepsilon S + kSM - a\mu^2(1+\delta^2) - \frac{1}{2}a\mu N(1+\delta\theta) - \frac{1}{2}a\chi\mu N(1-\delta\theta), \tag{11}$$

$$\frac{dN}{dt} = \frac{1}{2}a\mu^2(1+\delta^2) - \frac{1}{2}a\chi\mu N(1-\delta\theta), \tag{12}$$

$$\frac{dM}{dt} = a\mu^2(1+\delta^2) + \frac{1}{2}a\mu N(1+\delta\theta) - \frac{1}{2}a\chi\mu M(1-\delta\eta), \tag{13}$$

$$\frac{d\eta}{dt} = \frac{a\mu^2}{M}(2\delta - \eta - \eta\delta^2) + \frac{a\mu N}{2M}(\delta + \theta - \eta - \delta\theta\eta) + \frac{1}{2}a\chi\mu\delta(1-\eta^2), \tag{14}$$

$$\frac{d\theta}{dt} = \frac{a\mu^2}{2N}(2\delta - \theta - \theta\delta^2) + \frac{1}{2}a\chi\mu\delta(1-\theta^2), \tag{15}$$

$$\frac{d\delta}{dt} = -\frac{2\varepsilon S\delta}{\mu} - \frac{kSM\delta}{\mu} + \frac{kfSM\eta}{\mu} - \frac{1}{2}a(1-\delta^2)(2\mu\delta + N\theta - \chi N\theta), \tag{16}$$

where $S_0$ is the rate at which substrate is added to the system. To a certain extent, these equations enable us to consider the evolution of total concentrations ($S$, $\mu$, $N$ and $M$) separately from the chiral purities of monomers and polymers ($\delta$, $\theta$, $\eta$).

*Steady-state solutions*

Such symmetric systems typically have a symmetric solution, as we show this system has; however, there is no guarantee that the symmetric solution is the solution which is manifested, since the presence of nonlinearity means that there may be multiple solutions (one symmetric, others appearing in pairs and being asymmetric). The symmetric solution may be unstable and some of the asymmetric ones stable. An aim of this study is to determine how small the fidelity parameter $f$ may be and still give rise to stable asymmetric solutions. Seeking a steady-state solution, one immediately sees the benefit of the formulation (10)–(16). The symmetric steady state has $\delta = 0 = \theta = \eta$ ($S$, $\mu$, $N$, $M$ being given by more complicated expressions).

However, for larger values of the fidelity parameter, $f$, which controls the amount of feedback which polymers exert on the breakdown of the substrate, there are two achiral

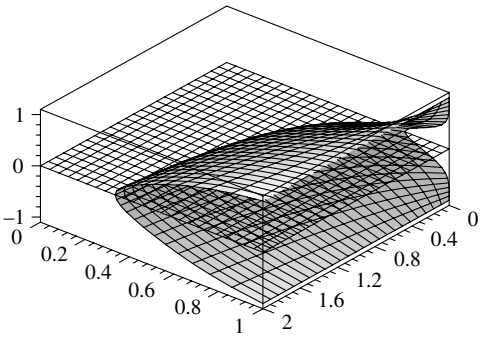


**Fig. 2.** Graph of the chiral purity $\delta$ against $\chi$ and $f$ for the steady-state values given by (17), for fidelity in the range $0 < f < 1$ and with $0 < \chi < 2$.

solutions. These two solutions form a pair of 'mirror image' solutions; in one, right-handed monomers and polymers dominate, the other is dominated by left-handedness. The crucial relationship linking the chiral purity (of monomers, $\delta$), fidelity ($f$) and the *relative* strength of enantiomeric cross-inhibition ($\chi$, being the ratio of the cross-inhibition rate $a\chi$ to the homochiral growth rate $a$) is

$$f = \left[\frac{1 + 10\delta^2 + 5\delta^4 + 2\chi(1-\delta^2)(1+3\delta^2)}{5 + 10\delta^2 + \delta^4 + 2\chi(1-\delta^2)(3+\delta^2)}\right] \times \left[\frac{4(1+\delta^2) + 2\chi(1-\delta^2)}{1 + 6\delta^2 + \delta^4 + 3\chi(1-\delta^4)}\right]. \tag{17}$$

Figure 2 illustrates the bifurcation structure. From this figure we see that when the inequality

$$f > f_c(\chi) := \frac{2(2+\chi)(1+2\chi)}{(5+6\chi)(1+3\chi)}, \tag{18}$$

is satisfied, there is an asymmetric steady-state solution which the system may approach. We can also view $\chi$ as a bifurcation parameter: provided $\frac{2}{9} < f < \frac{4}{5}$ then for small $\chi$ only the symmetric steady state exists, but as $\chi$ increases a bifurcation point ($\chi = \chi_c$) is traversed, and for $\chi > \chi_c$ the symmetric solution is unstable and two stable asymmetric steady states exist. As a function of $f$, the bifurcation point is at $\chi = \chi_c$, and is given by

$$\chi_c(f) = \frac{10 - 21f + \sqrt{81f^2 - 52f + 36}}{4(9f-2)}. \tag{19}$$

The steady-state solution has polymeric (number- and mass-weighted) concentrations of

$$N = \frac{\mu(1+3\delta^2)}{\chi(1-\delta^2)}, \quad M = \frac{\mu[1 + 10\delta^2 + 5\delta^4 + 2\chi(1-\delta^2)(1+3\delta^2)]}{\chi^2(1-\delta^2)^2}, \tag{20}$$

thus the average chain length $M/N$ is

$$\frac{M}{N} = 2 + \frac{1 + 10\delta^2 + 5\delta^4}{\chi(1-\delta^2)(1+3\delta^2)}. \tag{21}$$

https://doi.org/10.1017/S1473550405002454 Published online by Cambridge University Press

For the symmetric solution ($\delta=0$) we have an average chain length of $M/N=2+1/\chi$, thus long chains are particularly unlikely if $\chi$ is large. However, if $\chi$ is large enough for a symmetry-breaking solution to occur, then $\delta$ will be nearer $\pm1$ and so long homochiral chains are viable. For example, if we put $\delta=1-\nu$ with $\nu$ small then right-handed polymer chains dominate the system with average length $2/\nu\chi$. It is worth noting that in this case the system is also polymer-dominated: the monomer concentration $R_1$ is small (with $L_1$ even smaller and left-handed polymers even scarcer).

Another noteworthy property of an achiral steady-state solution is that the chiral purity of the polymers ($\theta$ and $\eta$) is always more extreme than that of the monomers ($\delta$)

$$\theta=\delta\left(\frac{3+\delta^2}{1+3\delta^2}\right),$$
$$\eta=\delta\left[\frac{5+10\delta^2+\delta^4+2\chi(1-\delta^2)(3+\delta^2)}{1+10\delta^2+5\delta^4+2\chi(1-\delta^2)(1+3\delta^2)}\right]. \tag{22}$$

Thus near symmetry ($\delta=0=\theta=\eta$) we have $\theta\approx3\delta$ and $\eta=(5+2\chi)\delta/(1+2\chi)$. Near chiral purity we have $\delta=1-\nu$ with $\nu$ small, implying $\theta=1-\frac{1}{4}\nu^3$ and $\eta=1-\frac{1}{4}\chi\nu^4$. Thus, if the monomers are as much as $\sim10\%$ away from chiral purity ($\delta=0.9$) the polymers will be only $\sim0.1\%$ away from purity.

*Stability of the steady-state solutions*

To investigate whether the chiral solution is preferred over the symmetric solution, we need to perform a stability analysis of the steady-state solution. We assume that $S$, $\mu$, $M$, $N$ are given by their steady-state values, and that $\delta$, $\theta$, $\eta$ are all small but perturbed away from zero. We then investigate whether the perturbations $\delta$, $\theta$, $\eta$ grow or decay. Linearizing (14)–(16) about the zero solution we obtain

$$\frac{d}{dt}\begin{pmatrix}\eta\\ \theta\\ \delta\end{pmatrix}=\frac{1}{2}a\mu\chi\begin{pmatrix}-1 & \dfrac{1}{(1+2\chi)} & \dfrac{2(1+3\chi)}{(1+2\chi)}\\ 0 & -1 & 3\\ \dfrac{f(1+3\chi)}{\chi^2} & \dfrac{\chi-1}{\chi^2} & -\dfrac{(1+5\chi)}{\chi^2}\end{pmatrix}\begin{pmatrix}\eta\\ \theta\\ \delta\end{pmatrix}. \tag{23}$$

An analysis of this system shows that if $f>f_c(\chi)$ (given by (18)) then the symmetric solution is unstable. This steady-state analysis shows that when the enantiomeric cross-inhibition ($\chi$) is large, the bifurcation to an asymmetric solution occurs at moderate values of the fidelity parameter $f$ (for example, $f>\frac{2}{9}$). However, when $\chi$ is small then a chiral imbalance is observed only when $f$ is very close to unity, in the limit of small $\chi$ we require $f>\frac{4}{5}$.

*Kinetics of the growing solution*

Differences between small and large cross-inhibition are also observed in the kinetics of the solution as we now show. Let us consider the system initiated from a state in which all concentrations are zero and follow the temporal evolution of the concentrations as the substrate accumulates, gives rise to monomers and ultimately polymers. The presence of a small parameter $\varepsilon$ in (4) means that we can find an approximate solution using the method of matched asymptotic expansions. We consider just the system of equations for the substrate, monomer and polymers, that is (10)–(13). We assume that the system remains in a symmetric state as it evolves, that is $\delta=0=\theta=\eta$ for all time – such a solution certainly exists. For the moment we ignore perturbations, although these will be considered later as we examine the stability of such a solution (see section entitled 'Kinetic stability'). We analyse the cases $\chi\gg1$ and $\chi\ll1$ separately.

*Large enantiomeric cross-inhibition ($\chi\gg1$)*

This is the simpler case to analyse, there being only three timescales of interest. The system starts with a long timescale, where $t=\mathcal{O}(\varepsilon^{-1/5})$, the concentrations of monomers being small, that of polymers being very small, whilst the substrate concentration grows linearly to a large size, up to $\mathcal{O}(\varepsilon^{-1/5})$. The timescale ends abruptly (at $t=t_{1c}\varepsilon^{-1/5}$) as the concentrations of monomer and polymer suddenly rise due to the feedback mechanism becoming active at larger polymer concentrations.

There follows a second, very rapid, timescale, in which all concentrations are large for a short time (formally in this timescale $t=t_{1c}\varepsilon^{-1/5}+\varepsilon^{1/5}t_2$ with $t_2=\mathcal{O}(1)$). At the end of this timescale the concentrations of all quantities decay slowly (in proportion to $1/t_2$) towards their steady-state magnitude. Over the third timescale, all concentrations evolve towards their precise steady-state values (here, $t=t_{1c}\varepsilon^{-1/5}+\mathcal{O}(1)$). A solution in this parameter regime is illustrated in Fig. 3.

*Small enantiomeric cross-inhibition ($\chi\ll1$)*

When there is little enantiomeric cross-inhibition, the structure of the asymptotic solution takes on a different form. The first timescale is identical to that above: with $t=\mathcal{O}(\varepsilon^{-1/5})$, the substrate concentration grows large, with a small monomer concentration and a smaller polymer concentration, both of which grow rapidly at the end of the timescale, leading to its abrupt end. The second timescale is again fast and all concentrations are large. However, in this case it ends with only the monomer and substrate concentrations decaying to a smaller size ($\mu$ and $S$), while the polymer concentrations ($N$ and $M$) remain large. A third timescale follows, which is also rapid, during which the monomer and substrate concentrations stabilize at small values. The fourth timescale is a further long timescale, over which the number of polymers and the mass in polymers slowly reduce (but the average polymer length ($M/N$) increases). Finally, over a fifth timescale, all concentrations approach their steady-state values. An example of this solution is given in Fig. 4.

*Kinetic stability*

In the preceding section, we have described the approximate solution for the quantities $S(t)$, $\mu(t)$, $N(t)$ and $M(t)$ governed by (10)–(13) in the case where $\delta=\theta=\eta=0$. Now we assume that $S(t)$, $\mu(t)$, $N(t)$ and $M(t)$ are given by this approximate

https://doi.org/10.1017/S1473550405002454 Published online by Cambridge University Press

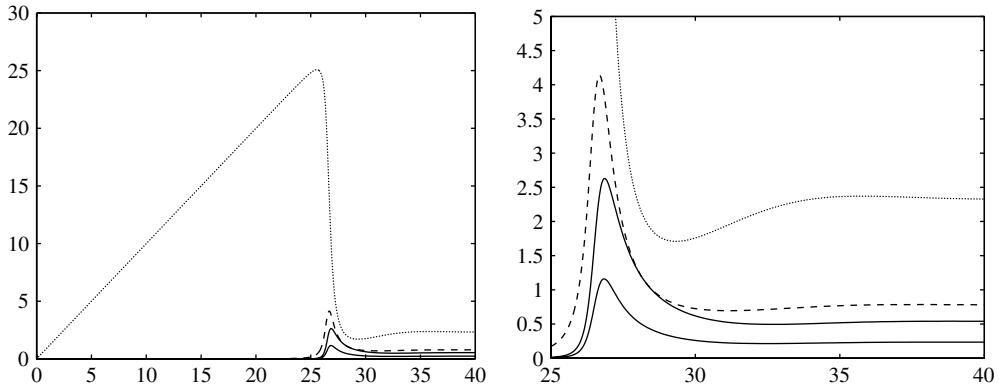

**Fig. 3.** Plot of a numerical solution of $S$, $\mu$, $N$, and $M$ against time for the case $\varepsilon = 10^{-5}$, $a = 1$, $k = 0.8$, $S_0 = 1$, $\chi = 3.333$. The dotted curve corresponds to $S(t)$, the dashed curve to $\mu(t)$, the upper solid curve to $M(t)$ and the lower solid curve to $N(t)$. The first timescale corresponds to the region $0 < t \lesssim 27$, the second around $t \approx 27$–$28$ and the third to larger values of $t$.

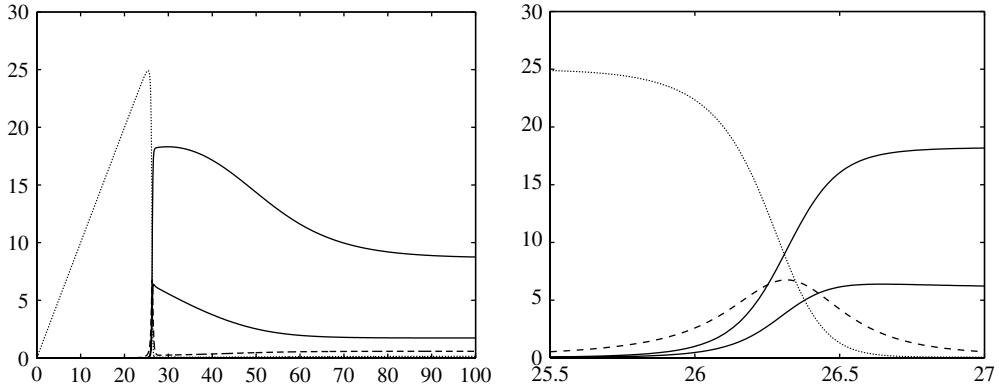

**Fig. 4.** Plot of numerical solution of $S(t)$ (the dotted curve), $\mu(t)$ (the dashed curve), $N(t)$ (the lower solid curve) and $M(t)$ (the upper solid curve). All parameters are as in Fig. 3 except $\chi = 0.333$. The first timescale occupies the region $0 < t \lesssim 25$, the second and third correspond to $25.5 < t < 27$ and are illustrated in the graph on the right. Timescale four can be seen on the left-hand graph, it corresponds to $27 < t \lesssim 60$ and the fifth and final timescale relates to $t \gtrsim 60$.

solution, but that at some particular point in time, $\delta$, $\theta$ and $\eta$ are perturbed away from zero by a small amount. We investigate the stability of the resulting system of equations for $\delta$, $\theta$ and $\eta$, that is, we ask whether the perturbation will decay ($\delta$, $\theta$, $\eta \to 0$) as time increases or whether the perturbation will grow. Linearizing about the solution $\delta = \theta = \eta = 0$, we obtain

$$\frac{d}{dt}\begin{pmatrix}\eta\\ \theta\\ \delta\end{pmatrix} = \frac{1}{2}a\mu(t) \times \begin{pmatrix} -\frac{2\mu}{M} - \frac{N}{M} & \frac{N}{M} & \chi + \frac{4\mu}{N} + \frac{N}{M} \\ 0 & -\frac{\mu}{N} & \chi + \frac{2\mu}{N} \\ \frac{2kfSM}{a\mu^2} & \frac{(\chi-1)N}{\mu} & -2 - \frac{2kSM}{a\mu^2} \end{pmatrix}\begin{pmatrix}\eta\\ \theta\\ \delta\end{pmatrix}. \quad (24)$$

The eigenvalues of the matrix determine the stability properties of the system. In each timescale, we obtain the critical value for $f$, namely $f_k$, above which ($f > f_k$) the perturbation will grow. These critical values are given in Table 1 for each timescale and in the two cases of small and large cross-inhibition.

Note that the threshold for this kinetic instability ($f_k$) is, in general, different from $f_c$ (18). In the first timescale, whatever value $\chi$ takes, the instability threshold is $f > f_k = \frac{1}{2}$. For small cross-inhibition the threshold increases in timescale II (that is $f_k > \frac{1}{2}$), and in timescales III and IV remains with $f_k > \frac{1}{2}$ before reaching the steady-state critical value of $f_k = \frac{4}{5}$. Qualitatively it appears that the instability becomes harder to sustain as the reaction proceeds. If $f < \frac{1}{2}$ then the system is always symmetric, that is in an achiral state. For $\frac{1}{2} < f < \frac{4}{5}$, early on in the polymerization process a chiral imbalance may form and persist for a short while, but later in the process the imbalance will be reduced and a symmetric solution will be regained. If $f > \frac{4}{5}$ then a perturbation at any stage of the process will grow and persist for all times; this means that an achiral state will form and an excess of one handedness over the other will be observed.

https://doi.org/10.1017/S1473550405002454 Published online by Cambridge University Press

Table 1. *Table of fidelity values where the kinetic instability occurs; that is the quoted values are $f_k$, where the symmetric solution is unstable for $f>f_k$*

| Timescale | $\chi<\chi_c$ | $\chi>\chi_c$ |
|---|---|---|
| TI | $f>f_k=\frac{1}{2}$ | $f>f_k=\frac{1}{2}$ |
| End TII | $f>f_k=\frac{1}{2(1-kM/aN)}$ | $f>f_k=\frac{2}{15}$ |
| TIII and TIV | $f>f_k=\frac{N}{N+\chi M}$ | |
| SSS | $f>f_k=f_c\sim\frac{4}{5}-\frac{34}{25}\chi$ | $f>f_k=f_c\sim\frac{2}{9}+\frac{8}{27}\chi^{-1}$ |

When cross-inhibition is large, the fidelity threshold $f_k$ reduces from $\frac{1}{2}$ to $\frac{2}{15}$ at the end of the second timescale, and then rises again, to $\frac{2}{9}$ for the steady state. Thus for $f<\frac{2}{15}$, the chirally selective feedback is so weak that a chiral imbalance can never be sustained, a perturbation at any stage of the polymerization process will decay and the system will return to a symmetric state. At the opposite extreme, if $f>\frac{1}{2}$ then a chiral perturbation at any stage of the process will be amplified and persist for all time. In between these two extremes there are two intermediate cases: when $\frac{2}{15}<f<\frac{2}{9}$, a perturbation will be damped in the first timescale, but in the short second timescale a perturbation would grow (albeit briefly as it is a rapid timescale), before being damped out as the system approaches the steady state. In the case of $\frac{2}{9}<f<\frac{1}{2}$ then any perturbation in the first timescale will again be damped, but one introduced in the second or third timescales will be amplified and persist for all later times.

*Summary*

In this model the nonlinear feedback mechanism occurs from the selective way in which chirally pure homopolymers influence the breakdown of the achiral substrate $S$ into chiral monomers. Once there is an excess of one handedness of chiral polymers, this produces more monomers of that chirality, and so the instability in the system self-perpetuates. Owing to the dual role of monomers – whereby they act both as growing units for homopolymers of their own chirality and growth inhibitors of the opposite chirality – monomers of the subdominant handedness are more likely to be used up in poisoning the more common handedness than forming homopolymers of their own chirality. Hence a return to the symmetric state is unlikely once a bifurcation has taken place.

More subtly, we note that the stability region (in parameter space) for the steady-state solution (18) illustrated in Fig. 2 and given by the last line of Table 1 is not the same as the stability regions for the kinetic solution (given in the first three lines of Table 1). Furthermore, the kinetic solution has different stability criteria at different stages of the reaction. We note, however, a consistency in that in all the results, a large enantiomeric cross-inhibition is more favourable for symmetry breaking than a small cross-inhibition.

## The origin of the RNA world

To address the problem of 'where did the RNA world come from?', we propose a detailed microscopic model of the kinetics of RNA polymerization and self-replication. Rather than assume the existence of closed catalytic hypercycles as Eigen (1971), Eigen and Schuster (1979), and Nuno *et al.* (1993) have done, we allow open-ended catalytic networks. To model the development of an RNA world we introduce the notation $C_r^\gamma$ to denote a chain of nucleotide bases of length $r$ and sequence $\gamma$. The four nucleotide bases adenosine (A), cytosine (C), guanine and thymine (T) are thus denoted by $C_1^{\mathrm{A}}$, $C_1^{\mathrm{C}}$, $C_1^{\mathrm{G}}$ and $C_1^{\mathrm{U}}$; a generic single-element sequence may be denoted by $C_1^\psi$. An exemplar single-strand RNA pentamer sequence is $C_5^{\mathrm{UACGG}}$. We use one of $\gamma$, $\theta$ and $\xi$ to denote a whole sequence of bases A, C, G, U, and a star to denote the Watson–Crick complement; thus if $\gamma=\mathrm{UACGG}$ then $\gamma^*=\mathrm{AUGCC}$.

*Detailed microscopic model*

The main reactions that such chains can undergo are as follows.

(i) Basic chain growth

$$C_r^\gamma+C_1^\psi\overset{\text{slow}}{\rightleftharpoons}C_{r+1}^{\gamma+\psi}, \tag{25}$$

which is in effect a Becker–Döring process and we assign this process the small rate coefficient $\varepsilon$.

(ii) Template-based chain synthesis (in which the Watson–Crick base-pairing of ribonucleotides on complementary chains gives rise to a catalytic effect)

$$C_r^\gamma+C_1^\psi+C_s^\theta\overset{\text{fast}}{\rightleftharpoons}C_{r+1}^{\gamma+\psi}+C_s^\theta. \tag{26}$$

While this effect occurs for all chains $\theta$, we expect some polymers ($C_s^\theta$ to be more effective catalysts than others (for example, $s>r$). This depends on how well the chains $\gamma$ and $\theta$ interact. We shall assume that in general this effect has some average effect, to which we shall assign the rate $\psi$; and when the sequence $\theta$ is the Watson–Crick complement of $\gamma+\psi$ we assign the process some larger reaction rate constant $\alpha$. (Note the change in notation here: $\chi$ no longer refers to a cross-inhibition effect as it did in (7).)

(iii) Inhibition or 'poisoning' whereby two polymer chains form a tightly bound duplex

$$C_r^\gamma+C_s^\theta\rightleftharpoons P_{r,s}^{\gamma,\theta}. \tag{27}$$

We neglect this effect in our present models. However, by comparing this model with that of chiral polymerization, we note the similarity between this mechanism and that of enantiomeric cross-inhibition (7), since the poisoned complex $P_{r,s}^{\gamma,\theta}$ cannot grow any further. When poisoning involves one copy of a potentially successful chain and one copy of a less successful chain, it causes a greater relative concentration drop of less successful chains than dominant ones; thus, it provides a mechanism for preventing the replication of less successful chains.

(iv) Hydrolysis, in which a long chain splits into two shorter chains. Chemically this corresponds to the reaction

$$C_{r+s}^{\gamma+\theta}\rightarrow C_r^\gamma+C_s^\theta, \tag{28}$$

https://doi.org/10.1017/S1473550405002454 Published online by Cambridge University Press

with rate constant $\eta$. This increases the number of chains but reduces the average chain length. At first sight this process appears detrimental to the formation of long chains and is undoubtedly so if $\eta$ is too large; however, since growth is catalysed in this model, having a greater number of chains confers some beneficial influence on chain growth.

(v) Enzymatic replication, also known as replicase ribozymal activity, in which a third chain ($C_s^{\xi}$ aids the growth of a chain ($C_r^{\gamma}$ which is already in close contact with another chain ($C_{r+k}^{\gamma^*+\theta^*}$) acting as a template

$$C_r^{\gamma} + C_1^{\psi} + C_{r+k}^{\gamma^*+\theta^*} + C_s^{\xi} \rightleftharpoons C_{r+1}^{\gamma+\psi} + C_{r+k}^{\gamma^*+\theta^*} + C_s^{\xi}. \qquad (29)$$

Cech was awarded the Nobel prize for the discovery of this kind of process in RNAs (Kruger *et al.* 1982). Here the combination of $\gamma$ with $\psi$ is a subsequence of the chain $\gamma+\theta$ (that is $\gamma+\psi$ is a subset of $\gamma+\theta$) while $C_s^{\xi}$ plays the role of a replicase ribozyme. Needless to say, some of these replicases will have much higher efficiency than (most) of the others. We shall assign the rate constant $\zeta$ to this mechanism.

As already noted we will be ignoring inhibition (mechanism (iii)) and for the moment we shall also ignore hydrolysis (iv), although this will be introduced later (see the subsection on a more refined macroscopic model). The remaining effects ((i), (ii), (v)) are all of Becker–Döring form. Thus we define $c_r^{\gamma}(t)$ as the concentration of $C_r^{\gamma}$ and obtain the kinetic equations

$$\frac{dc_r^{\gamma}}{dt} = J_{r-1}^{\gamma_l,\,-\gamma_l+\gamma} + J_{r-1}^{\gamma-\gamma_r,\,\gamma_r} - \sum_{\psi=\mathrm{A,C,G,U}} (J_r^{\psi,\gamma} + J_r^{\gamma,\psi}). \qquad (30)$$

The duplication of terms is due to the polymers being allowed to grow at both ends. The quantities $\gamma_1$ and $\gamma_r$ represent the first and last elements of the sequence $\gamma$. The expression $\gamma-\gamma_r$ represents the first $(r-1)$ elements of $\gamma$ (that is, all of $\gamma$ except for the last element), while $-\gamma_1+\gamma$ denotes the whole of $\gamma$ except for the first element.

The fluxes $J_r^{\gamma,\psi}$ denote the rate at which the RNA polymer sequence $\gamma$ grows due to the addition of the monomeric nucleotide $\psi$

$$J_r^{\gamma,\psi} = \left(c_r^{\gamma}c_1^{\psi} - \frac{\bar{c}_r^{\gamma}\,\bar{c}_1^{\psi}}{\bar{c}_{r+1}^{\psi,\gamma}}c_{r+1}^{\psi,\gamma}\right) \times \left(\varepsilon + \alpha c_{r+1}^{\gamma,\psi} + \chi\sum_{s,\theta} c_s^{\theta} + \zeta c_{r+1}^{\gamma,\psi}\sum_{s,\theta} c_s^{\theta}\right). \qquad (31)$$

Here, $\bar{c}_r^{\gamma}$ denotes the equilibrium value of $c_r^{\gamma}$; a similar formula holds for $J_r^{\psi,\gamma}$.

From here on, we shall assume that a chain and its complement have identical concentrations. This enables the template-based growth (ii) to be described by an *autocatalytic* rather than a cross-catalytic term, autocatalysis being easier to analyse mathematically. Thus instead of $C_r^{\gamma^*}$ catalysing the production of $C_r^{\gamma}$, with the assumption that the concentrations $C_r^{\gamma}=c_r^{\gamma^*}$, in the mathematical model we effectively have $c_r^{\gamma}$ catalysing its own growth. Since the rates $\varepsilon$, $\alpha$, $\chi$, $\zeta$ and $\eta$ are not dependent on the sequence, this assumption will hold for all time if it holds at $t=0$.

Table 2. *Illustration of numbering the different polymers sequences of length $\Lambda=10$. There are $N=4^{10}=1\,048\,576$ different RNA sequences that can be formed. In (32) these are indexed by the symbol n*

| *n* | Sequencer |
|---|---|
| 1 | AAAAAAAAAA |
| 2 | AAAAAAAAAC |
| 3 | AAAAAAAAAG |
| 4 | AAAAAAAAAU |
| 5 | AAAAAAAACA |
| 6 | AAAAAAAACC |
| ⋮ | ⋮ |
| 262 144 | AUUUUUUUUU |
| 262 145 | CAAAAAAAAA |
| ⋮ | ⋮ |
| 1048 575 | UUUUUUUUUG |
| 1048 576 | UUUUUUUUUU |

*A macroscopic model*

In previous modelling work where the formation of micelles and vesicles has been of interest (Coveney & Wattis 1996, 1998), we have used a coarse-graining technique to obtain results at a macroscopic level which can be compared with experimental data. In this technique the aggregation space is sampled at only a few sizes. In the current work this corresponds to retaining only a small set of polymer lengths; for example, $r=1$, 10, 20 instead of $r=1, 2, \ldots$ . This coarse-graining technique is systematic but approximate; it has been shown to be asymptotically exact in various cases (Wattis & King 1998) and is being refined (Bolton & Wattis 2003).

In one extreme coarse-grained limit, we focus on polymers of just one length $\Lambda\in\mathbb{N}$, and ignore all longer lengths (we effectively assume their concentrations are all zero), while all shorter lengths are also ignored (that is, $r=2$, 3, …, $\Lambda-1$). A new flux function which describes how $\Lambda$ monomers combine in a single step to form a polymer is then constructed. This polymer will be denoted by $X_{\Lambda}^{\gamma}$ where the subscript $\Lambda$ denotes that it is composed of $\Lambda$ monomers and the superscript $\gamma$ represents the sequence of monomers in the chain (for examples of $\gamma$ in the case of $\Lambda=10$, see Table 2). The kinetic equations (30) and (31) are then replaced by

$$\frac{dy_n}{dt} = 2(x_1^{\Lambda} - \beta y_n)\left(\varepsilon + \alpha y_n + \chi\sum_{p=1}^{N} y_p + \zeta y_n\sum_{p=1}^{N} y_p\right)^{\lambda}, \qquad (32)$$

where $x_1$ is the monomer concentration, which we have assumed is the same for all four monomer types, and $\lambda=\Lambda-1$. The variables $\{y_n\}_{n=1}^{N}$ describe the concentrations of the $N=4^{\Lambda}$ different possible sequences of polymers of length $\Lambda$, i.e. $n$ enumerates the sequences $\gamma$. The case of $\Lambda=10$ is illustrated in Table 2 where the similarity with counting in base four is apparent, the symbols A, C, G, U being replacements for 0, 1, 2, 3. Working back from the kinetic equation (32) it is possible to deduce the

https://doi.org/10.1017/S1473550405002454 Published online by Cambridge University Press

Table 3. *The four effective rate processes by means of which chains are formed in our macroscopic model* (*32*). *Reprinted with permission from J. Phys Chem. B* **103**, *4231*, © *1999 American Chemical Society*

| | |
|---|---|
| $\Lambda X_1 \rightleftharpoons X^{\chi}_{\Lambda}$ | Uncatalysed, with forward rate coefficient $=\varepsilon$ |
| $\Lambda X_1 + X^{\chi}_{\Lambda} \rightleftharpoons 2X^{\chi}_{\Lambda}$ | Autocatalysis, with forward rate coefficient $=\alpha$ |
| $\Lambda X_1 + X^{\theta}_{\Lambda} \rightleftharpoons X^{\chi}_{\Lambda} X^{\theta}_{\Lambda}$ | Cross-catalysis, with forward rate coefficient $=\chi$ |
| $\Lambda X_1 + X^{\chi}_{\Lambda} + X^{\theta}_{\Lambda} \rightleftharpoons 2X^{\chi}_{\Lambda} + X^{\theta}_{\Lambda}$ | Enzymatic catalysis, with forward rate coefficient $=\zeta$ |

coarse-grained chemical processes which they describe. These are given in Table 3.

*The symmetric solution*

As an example we solve (32) in the case of irreversible polymerization (which implies $\beta=0$) and a constant monomer concentration (for simplicity we put $2x_1^{\Lambda}=1$). An approximate solution to the kinetic equations (32) can be found given the assumption that all chains occur with equal concentrations, that is, $y_n(t)=Y(t)$, independent of $n$. This symmetry Ansatz leads to

$$Y(t)=\frac{\varepsilon}{(\alpha+N\chi)}\left[\frac{1}{(1-t/t_c)^{1/(\lambda-1)}}-1\right],$$
$$\text{where } t_c=\frac{\varepsilon^{1-\lambda}}{(\lambda-1)(\alpha+N\chi)}. \tag{33}$$

This solution is valid until $Y(t)$ reaches $\mathcal{O}(1)$, when the enzymatic reaction mechanism becomes significant and an alternative approximation is required. As with the first timescale of the chiral polymerization solution (see the earlier section on the kinetics of the growing solution), this approximation describes slow kinetics occurring over a large interval of time. This timescale also has an abrupt end: as $t$ approaches $t_c$ catalytic effects start to dominate the uncatalysed reaction mechanisms.

*Kinetic stability*

Even from the early-time solution (33) we can demonstrate an instability of the symmetric solution. We consider a small $n$-dependent perturbation $\hat{y}_n(t)$, where $y_n(t)=Y(t)(1+\hat{y}_n(t))$ with $\sum_n \hat{y}_n(t)=0$ so that some chains have greater concentrations than others. The perturbations $\hat{y}_n(t)$ then evolve according to

$$\frac{d\hat{y}_n}{dt}=\frac{\hat{y}_n(t)B(t)^{\lambda-1}}{Y(t)}[\lambda Y(t)(\alpha+\zeta N Y(t))-B(t)], \tag{34}$$

where $B(t)=\varepsilon+\alpha Y(t)+\chi N Y(t)+\zeta N Y(t)^2$. Now if $\alpha > N\chi/(\lambda-1)$ then the perturbations $\hat{y}_n(t)$ will grow in amplitude at times $t>t_i$, where

$$t_i=\left\{1-\left[1-\left(\frac{\alpha+N\chi}{\alpha\lambda}\right)\right]^{\lambda-1}\right\}\frac{\varepsilon^{1-\lambda}}{(\lambda-1)(\alpha+N\chi)}. \tag{35}$$

Note that $t_i<t_c$ so there is a large interval of time $t_i<t<t_c$ during which perturbations will develop. Unfortunately, the linear equation (34) does not yield an expression which links the 'shape' of perturbation in $n$-space with a growth rate. If we assume a separable solution for $\hat{y}_n(t)$ of the form $\hat{y}_n(t)=T(t)\omega_n$ then $T(t)$ is determined, but $\omega_n$ is not, that is, all perturbations $\omega_n$ have the same growth rate. A higher-order analysis is required to determine the most unstable shape mode. Intuitively we expect a few chains to flourish, and in our model the chains which prosper will depend on non-uniformities in initial data. Other chains will remain at low concentrations due to competition for the available monomers from the flourishing chains. In the real world, the autocatalytic, cross-catalytic and enzymatic rates will have some dependence on the precise sequence of nucleotides in the polymeric chain, and these variations in rate constants will also have a role in determining which chains replicate at the fastest rate.

This illustration shows that symmetry-breaking occurs in our account of the origins of the RNA world with a similar mechanism to that in chiral polymerization. However, this model has only used three of the five mechanisms identified at the start of this section. Given that the inhibition mechanism (mechanism (iii)) is similar in effect to enantiomeric cross-inhibition in chiral polymerization, we have some confidence that inhibition will not destroy the symmetry-breaking phenomenon in our model of RNA sequence formation. To include hydrolysis in our model we need a less severe approximation of (30) and (31).

*A more refined macroscopic model*

We now consider another coarse-graining approximation of (30)–(31). Instead of retaining just monomers and one length of polymer, we now keep two lengths of polymer, namely $\Lambda$ and $2\Lambda$ For shorter chains (length $\Lambda$), we retain the same notation as used above, namely $y_n$ ($1\leqslant n\leqslant N=4^{\Lambda}$). For the longer chains, we use the notation $Y_{m,n}$ to represent a chain for which the first $\Lambda$ sites exactly correspond to that of $Y_m$ and for which the second $\Lambda$ sites correspond to $Y_n$. Thus $Y_{m,n}$ can be viewed as a simple concatenation of $Y_m$ and $Y_n$. The concentrations of these quantities are referred to by $y_{m,n}(t)$, $y_m(t)$ and $y_n(t)$. For simplicity, we retain $x_1$ as the monomer concentration – fixed at the same value for all four nucleotide monomers. Hydrolysis then corresponds to the splitting of a long chain into two shorter ones via $Y_{m,n}\rightarrow Y_m+Y_n$, with a rate constant $\eta$. An additional benefit of this model is that a longer chain of the form $Y_{m,n}$ catalyses the growth of both the shorter chains $Y_m$ and $Y_n$

https://doi.org/10.1017/S1473550405002454 Published online by Cambridge University Press

Table 4. *Reactions include in the model* (36) *and* (37), *together with their corresponding forward rate constants. Subscripts* '*S*' *and* '*L*' *denote short and long chains, respectively. Reprinted with permission from J. Phys. Chem. B* **103**, *4231*, *© 1999 American Chemical Society*

| | | |
|---|---|---|
| $\Lambda X_1 \to Y_n$ | $\varepsilon_S$ | Uncatalysed polymerization |
| $Y_n + \Lambda X_1 \to Y_{n,m}$ | $\varepsilon_L$ | Uncatalysed growth of long from short chains |
| $Y_n + \Lambda X_1 \to 2Y_n$ | $\alpha_S$ | Autocatalysis of short chains |
| $Y_{m,n} + Y_m + \Lambda X_1 \to 2Y_{m,n}$ | $\alpha_L$ | Autocatalysis of long chains |
| $Y_{m,n} \to Y_m + Y_n$ | $\eta$ | hydrolysis |
| $Y_m + \Lambda X_1 \to Y_m + Y_n$ | $\chi_S$ | Cross-catalysis of short by short chains |
| $Y_{m,n} + Y_k + \Lambda X_1 \to Y_{m,n} + Y_{k,l}$ | $\chi_L$ | Cross-catalysis of long by long chains |
| $Y_{m,n} + \Lambda X_1 \to Y_{m,n} + Y_k$ | $\chi_X$ | Cross-catalysis of short by long chains |
| $Y_{p,q} + Y_n + \Lambda X_1 \to 2Y_n + Y_{p,q}$ | $\zeta_{SS}$ | Ribozymic synthesis of short chains |
| $Y_{p,q} + Y_{m,n} + \Lambda X_1 \to Y_n + Y_{m,n} + Y_{p,q}$ | $\zeta_{SL}$ | Ribozymic synthesis of short chains |
| $Y_{p,q} + Y_{n,m} + \Lambda X_1 \to Y_n + Y_{n,m} + Y_{p,q}$ | $\zeta_{SL}$ | Ribozymic synthesis of short chains |
| $Y_{p,q} + Y_{m,n} + Y_m + \Lambda X_1 \to 2Y_{m,n} + Y_{p,q}$ | $\zeta_{LL}$ | Ribozymic synthesis of long chains |
| $Y_{p,q} + Y_{m,n} + Y_n + \Lambda X_1 \to 2Y_{m,n} + Y_{p,q}$ | $\zeta_{LL}$ | Ribozymic synthesis of long chains |

into $Y_{m,n}$.

$$\begin{aligned}\frac{dy_n}{dt} = x_1^{\Lambda}\Bigg(&\varepsilon_S + \alpha_S y_n + \sum_{m=1}^{N}\chi_S y_m + \sum_{p,q=1}^{N,N}\chi_X y_{p,q} + \sum_{p,q=1}^{N,N}\zeta_{SS} y_{p,q} y_n \\ &+ \sum_{m,p,q=1}^{N,N,N}\zeta_{SL} y_{p,q}(y_{m,n} + y_{n,m})\Bigg)^{\lambda} + \sum_{m=1}^{N}\eta(y_{m,n} + y_{n,m}) \\ &- \sum_{m=1}^{N} x_1^{\Lambda} y_n\Bigg(\varepsilon_L + \alpha_L y_{m,n} + \sum_{p,q=1}^{N,N}\chi_L y_{p,q} \\ &+ \sum_{p,q=1}^{N,N}\zeta_{LL} y_{m,n} y_{p,q}\Bigg)^{\Lambda} - \sum_{m=1}^{N} x_1^{\Lambda} y_n(\varepsilon_L + \alpha_L y_{n,m} \\ &+ \sum_{p,q=1}^{N,N}\chi_L y_{p,q} + \sum_{p,q=1}^{N,N}\zeta_{LL} y_{n,m} y_{p,q}\Bigg)^{\Lambda}\end{aligned} \tag{36}$$

$$\begin{aligned}\frac{dy_{m,n}}{dt} = &-\eta y_{m,n} + \left(x_1^{\Lambda} y_m + x_1^{\Lambda} y_n\right)\Bigg(\varepsilon_L + \alpha_L y_{m,n} \\ &+ \sum_{p,q=1}^{N,N}\chi_L y_{p,q} + \sum_{p,q=1}^{N,N}\zeta_{LL} y_{m,n} y_{p,q}\Bigg)^{\Lambda}.\end{aligned} \tag{37}$$

Here we have once again made the assumption that polymerization is irreversible. Note that even the first line of the equation for $Y_n$ is more complex than (32) due to the various forms of enzymatic replication (mechanism (v)) which require a long chain to act enzymatically and either a short or a long chain to act as a template. These two possible templates are assigned possibly different rate constants ($\zeta_{SS}$ or $\zeta_{SL}$). The spontaneous (slow) polymerization rates of short and long polymers are assigned small, but potentially different, rates $\varepsilon_S$, $\varepsilon_L$. Similarly, different autocatalytic and cross-catalytic rates are denoted by $\alpha_S$, $\alpha_L$, $\chi_S$, $\chi_L$ and $\chi_X$; with $\chi_X$ being the rate at which long chains cross-catalyse the formation of short chains. These mechanisms and associated rate constants are summarized in Table 4. Other simplifying assumptions could be made, such as $y_{m,n}(t) = y_{n,m}(t)$; however, the system is now in a form where it is possible to analyse the kinetic stability of the uniform (symmetric) solution.

*Symmetric solution*

We first determine the symmetric solution; for this there are just two variables to find, namely the short-chain concentration (the same concentration for each sequence), and the long-chain concentration. We denote these by

$$y_{m,n}(t) = Z(t), \qquad y_m(t) = Y(t); \tag{38}$$

when inserted into (36) and (37), these imply

$$\begin{aligned}\dot{Z} = &-\eta Z + 2^{1-2\Lambda} Y(\varrho - \Lambda N Y - 2\Lambda N^2 Z)^{\Lambda} \\ &\times(\varepsilon_L + \alpha_L Z + \chi_L N^2 Z + \zeta_{LL} N^2 Z^2)^{\Lambda}\end{aligned} \tag{39}$$

$$\begin{aligned}\dot{Y} = &2\eta N Z - 2^{1-2\Lambda} N Y(\varrho - \Lambda N Y - 2\Lambda N^2 Z)^{\Lambda} \\ &\times(\varepsilon_L + \alpha_L Z + \chi_L N^2 Z + \zeta_{LL} N^2 Z^2)^{\Lambda} \\ &+ 2^{-\Lambda}(\varrho - \Lambda N Y - 2\Lambda N^2 Z)^{\Lambda}(\varepsilon_S + \alpha_S Y + \chi_S N Y \\ &+ \chi_X N^2 Z + \zeta_{SS} N^2 Y Z + 2\zeta_{SL} N^3 Z^2)^{\lambda}.\end{aligned} \tag{40}$$

For this example we consider the case of a constant total concentration of ribonucleotides, that is we assume $\rho = 4x_1(t) + N\Lambda Y(t) + 2\Lambda N^2 Z(t)$ is constant. Although we cannot express the solution of (39) and (40) in terms of elementary functions, the system has a unique solution and we now examine its stability to perturbations.

*Kinetic stability*

To analyse the stability of the uniform (or symmetric) solution (38), we put

$$y_{m,n}(t) = Z(t) + Z(t)\hat{y}_{m,n}(t), \quad y_n(t) = Y(t) + Y(t)\hat{y}_n(t), \tag{41}$$

with $\hat{y}_n(t)$, $\hat{y}_{m,n}(t) \ll 1$. Inserting this into (36) and (37), we obtain a system of equations of the form

$$\frac{d\hat{y}_n}{dt} = A(t)\hat{y}_n + B(t)\sum_{m=1}^{N}(\hat{y}_{m,n} + \hat{y}_{n,m}) \tag{42}$$

$$\frac{d\hat{y}_{m,n}}{dt} = C(t)\hat{y}_{m,n} + D(t)[\hat{y}_m + \hat{y}_n], \tag{43}$$

https://doi.org/10.1017/S1473550405002454 Published online by Cambridge University Press

where $A(t)$, $B(t)$, $C(t)$ and $D(t)$ are given by complicated expressions involving $Y(t)$, $Z(t)$ and all the parameters from the model equations (36) and (37). Full details are given in Wattis & Coveney (1999). Since (42) and (43) form a linear problem for the variables $\hat{y}_n(t)$ and $\hat{y}_{m,n}(t)$, a separable solution can be found. To separate the temporal evolution and the $n$ and $(m, n)$ dependence, we put

$$\hat{y}_n(t)=\omega_n S_S(t), \quad \hat{y}_{m,n}(t)=\omega_{m,n} S_L(t), \tag{44}$$

so that the variables $\omega_m$ and $\omega_{m,n}$ determine the 'shape' of the perturbation in $(m, n)$ sequence space, and $S_S(t)$ and $S_L(t)$ describe the temporal evolution of the perturbation in the short and long chains, respectively. Although it is the latter quantities we are interested in, the two problems cannot be completely separated. To make further analytical progress, we are forced to invoke the assumption $\omega_{m,n}=K(\omega_m+\omega_n)$, where $K$ is a separation constant. Thus the problem for $S_S(t)$, $S_L(t)$ retains some information concerning the 'shape' functions $\omega_m$, $\omega_{m,n}$ through $K$,

$$\frac{d}{dt}\begin{pmatrix} S_S \\ S_L \end{pmatrix}=\begin{pmatrix} A(t) & 2NKB(t) \\ D(t)/K & C(t) \end{pmatrix}\begin{pmatrix} S_S \\ S_L \end{pmatrix}. \tag{45}$$

The Routh–Hourwitz criteria (Murray 1989) which specify the conditions under which the eigenvalues of the matrix have negative real parts imply $A+C<0$ and $AC>2NBD$. If these hold then the system is stable and $S_S$ and $S_L$ both decay with increasing time. To prove the formation of a patterned state in which some chains dominate others we have to prove either $A+C>0$ or $AC<2NBD$. Note that neither of these stability criteria depend on the separation constant $K$. Thus there is not one shape mode $(\omega_n, \omega_{m,n})$ which becomes unstable before the others, rather many shape modes become unstable at the same bifurcation point. Unfortunately we are in the same position as in the discussions following (34) and (35) earlier, in that we cannot describe the form of the solution just past the bifurcation point. As there, we expect there to be a subset of both short and long chains which prosper (the long chains being composed of two flourishing short chains, and if a chain is in this set of 'successful' replicators then so is its complement), other chains will remain at low concentrations due to the competition for a limited supply of nucleotide bases.

After developing approximations for the quantities $Y(t)$, and $Z(t)$ we deduce various criteria for the existence of an instability of the uniform solution. One such inequality is

$$\alpha_S > \frac{N(\Lambda\varepsilon_S+\varrho\chi_S)}{(\lambda-1)\varrho}, \tag{46}$$

which can be interpreted as a lower bound on the autocatalytic rate depending both on the spontaneous slow polymerization ($\varepsilon_S$) and on the cross-catalytic chain growth mechanism ($\chi_S$). This means that the accuracy of the templating mechanism (ii) must lie above a certain threshold. Analysis of the inequality $AC<2NBD$ shows that an instability can be triggered when $\eta$ lies above some threshold, that is when hydrolysis is strong enough.

*Summary*

We have proposed a model for RNA polymerization containing spontaneous, catalytic and enzymatic mechanisms of chain growth. The model includes information on the sequence of bases and is thus able to track information propagation through chain replication via (imperfect) templating. We have illustrated how the great complexity of the model (due to the numerous different sequences and chain lengths) can be reduced to a simpler system which is amenable to a theoretical analysis. For any particular chain length $N$ there are $4^N$ different possible sequences. If we consider a general model which contains all possible chain lengths up to length $N$, then there are $\frac{3}{4}(4^{N+1}-1)$ combinations. By using a coarse-graining contraction, we reduced the model so that we need only consider one (or in a more general model, two) chain lengths. Secondly, instead of considering all $4^N$ possible sequences $\gamma$, we have assumed that a chain and its Watson–Crick complement occur with equal frequency. This is an assumption which simplifies the structure of the differential equations and slightly reduces the number of variables in the model; the resulting system of equations still has $4^{N-1/2}$ variables. By examining the stability of the symmetric solution we have shown that there are regions of parameter space in which a spontaneous bifurcation will take place. This results in certain chains becoming much more numerous than others; thus small external perturbations may provide a mechanism for the initial selection of sequences which flourish and propagate and those which are unable to replicate due to the competition for a finite supply of nucleotide monomers. In reality, the full model may well exhibit more complex instabilities in which a chain and its complement have different concentrations. However, such a model would still suffer from the instabilities we have found in a reduced model.

Owing to the number and complexity of mechanisms in this model, there is no single parameter which can be interpreted as a 'fidelity' parameter in the chiral polymerization model. In that model, we saw that it was a combination of large fidelity ($f$) and enantiomeric cross-inhibition ($\chi$) which caused symmetry-breaking. Here, in RNA polymerization it is primarily a combination primarily of autocatalysis (the template-based chain synthesis of one chain by its complement at a rate which we have denoted by $\alpha$) and enzymatic replication ($\zeta$) which causes symmetry-breaking; however, the presence of hydrolysis ($\eta$) may also destabilize the uniform solution and cause a bifurcation.

## Conclusions

The two models we have analysed both include spontaneous but slow polymerization and some form of autocatalysis, which acts as a nonlinear feedback mechanism. The source of the nonlinearity differs in the two models: in chiral polymerization, the presence of homochiral polymers amplifies

https://doi.org/10.1017/S1473550405002454 Published online by Cambridge University Press

the rate at which a precursor substrate chemical is broken down into chiral monomers. In RNA polymerization the nonlinear feedback mechanism originates in the growth mechanisms of chains; sequences effectively catalyse their own production since we assume that a polymer sequence and its complement occur in equal concentrations.

Both models also display an element of competition: in chiral polymerization, chains compete for the monomers while the monomers have a dual role, being both agents of growth for polymers of their own handedness and inhibitors for opposite-handed polymers. In the RNA-world model there is also competition between polymeric chains for monomers, this time with chains having a dual role – growing themselves and acting as catalysts for the growth of other chains. In a more detailed model, chains would also play the role of inhibitor, which we have ignored here (mechanism (iii)). The inhibition mechanism which we have ignored in modelling the origin of the RNA world is analogous to enantiomeric cross-inhibition in Sandars' model of chiral polymerization (Sandars 2003). While at first sight this might appear to be a hindrance to the formation and persistence of an asymmetric solution, it is in fact be a driving force for the development of chirality, since it inhibits the growth of the chiral polymers of lower concentration to a greater extent that the more abundant chirality.

In both chiral polymerization and RNA self-replication there is a symmetric solution where both enantiomers, or chains of all compositions, occur with equal concentrations. Yet in both systems there are ranges of parameter values in which a small perturbation away from the symmetric state grows in time, leading to the more complex and more interesting solutions which are necessary for the emergence of life. This symmetry-breaking is most graphically seen in Fig. 2 where the steady-state solution of the chiral polymerization model is illustrated. However, we have shown that it is not just a steady-state feature, but that symmetry breaking occurs during the pre-steady kinetics: it may occur extremely early on in the polymerization process and persist until a steady state is achieved.

## Acknowledgements

We are grateful to Professor Pat Sandars for useful conversations concerning aspects of modelling chiral polymerization, JADW is grateful to Axel Brandenburg and Anja Andersen for organizing the Astrobiology meeting at Nordita in January 2005. PVC is grateful to Pier Luigi Luisi and Albert Eschenmoser for lively and stimulating discussions which led to the modelling of RNA polymerization. PVC is also grateful for financial support under EPSRC Reality Grid grant GR/R67699. We are both grateful to the Center for Advanced Mathematical Sciences at the American University of Beirut which ran a workshop on Dynamics and its Applications in 2002 where our work on chiral polymerization started. Finally, our thanks go to the referees for their constructive suggestions and encouraging comments.

## References

Becker, R. & Döring, W. (1935). Kinetische Behandung der Keimbildung in übersättigten Dämpfen. *Ann. Phys.* **24**, 719–752.

Bolton, C.D. & Wattis, J.A.D. (2003). Generalized coarse-grained Becker–Döring equations. *J. Phys. A: Math. Gen.* **36**, 7859–7888.

Brandenburg, A., Andersen, A.C., Höfner, S. & Nilsson, M. (2005a). Homochiral growth through enantiomeric cross-inhibition. *Origins Life Evol. Biosphere* **35**, 225–242.

Brandenburg, A., Andersen, A.C. & Nilsson, M. (2005b). Dissociation in a polymerisation model of homochirality. *Origins Life Evol. Biosphere* (in press) (arXiv.org/abs/q-bio/0502008).

Colonna, S., Fleischecker, G.R. & Luisi, P.L. (1994). *Self-production of Supramolecular Structures: from Synthetic Structures to Models of Minimal Living Systems* (*NATO ASI Series*). Kluwer, Dordrecht.

Coveney, P.V. & Wattis, J.A.D. (1996). Analysis of a generalized Becker–Döring model of self-reproducing micelles. *Proc. R. Soc. London* A **452**, 2079–2102.

Coveney, P.V. & Wattis, J.A.D. (1998). A Becker–Döring model of self-reproducing vesicles. *J. Chem. Soc.: Faraday Trans.* **102**, 233–246.

Coveney, P.V. & Wattis, J.A.D. (1999). Cluster renormalization for the Becker–Döring equations. *J. Phys. A: Math. Gen.* **32**, 7145–7152.

Eigen, M. (1971). Selforganization of matter and the evolution of biological macromolecules. *Naturwissenschaften* **58**, 465–523.

Eigen, M. & Schuster, P. (1979). *The Hypercycle. A Principle of Natural Self-organisation*. Springer, New York.

Joyce, G.F., Visser, G.M., van Boeckel, C.A.A., van Boom, J.H., Orgel, L.E. & van Westrenen, J. (1984). Chiral selection in poly(C)-directed synthesis of oligo(G). *Nature* **310**, 602–604.

Kruger, K., Grabowski, P.J., Zaug, A.J., Sands, J., Gottschling, D.E. & Cech, T.R. (1982). Self-splicing RNA – auto-excision and auto-cyclization of the ribosomal-RNA intervening sequence of Tetrahymena. *Cell* **31**, 147–157.

Murray, J.D. (1989). *Mathematical Biology, Biomathematics*, vol. 19. Springer, Berlin.

Nuno, J.C., Andrade, M.A., Moran, F. & Montero, F. (1993). A model of an autocatalytic network formed by error-prone self-replicative species. *Bull. Math. Biol.* **55**, 385–415.

Sandars, P.G.H. (2003). A toy model for the generation of homochirality during polymerisation. *Origins Life Evol. Biosphere* **33**, 575–587.

Sandars, P.G.H. (2005). Chirality in the RNA world and beyond. *Int. J. Astrobiol.* **4**, 49–61.

Wattis, J.A.D. & Coveney, P.V. (1999). The origin of the RNA world: a kinetic model. *J. Phys. Chem* B **103**, 4231–4250.

Wattis, J.A.D. & Coveney, P.V. (2005). Symmetry-breaking in chiral polymerisation. *Origins Life Evol. Biosphere* (in press) (arXiv.org/abs/0402091).

Wattis, J.A.D. & King, J.R. (1998). Asymptotic solutions of the Becker–Döring equations. *J. Phys. A: Math. Gen.* **31**, 7169–7189.

Zubay, G. (2000). *The Origins of Life on Earth and in the Cosmos*, 2nd edn. Academic Press, London.